

Model on picometer-level light gravitational delay in the GRACE Follow-On-like missions

Jin-Zhuang Dong(董金壮), Wei-Sheng Huang(黄玮圣), Cheng-Gang Qin(秦成刚), Yu-Jie Tan(谈玉杰), and Cheng-Gang Shao(邵成刚)

Citation: Chin. Phys. B, 2024, 33 (**11**): 110401. DOI: 10.1088/1674-1056/ad7af9
Journal homepage: http://cpb.iphy.ac.cn; http://iopscience.iop.org/cpb

What follows is a list of articles you may be interested in

Thermodynamics and weak cosmic censorship conjecture of charged AdS black hole in the Rastall gravity with pressure

Xin-Yun Hu(胡馨匀), Ke-Jian He(何柯健), Zhong-Hua Li(李中华), Guo-Ping Li(李国平)
Chin. Phys. B, 2020, 29 (**5**): 050401. DOI: 10.1088/1674-1056/ab7daa

The global monopole spacetime and its topological charge

Hongwei Tan(谭鸿威), Jinbo Yang(杨锦波), Jingyi Zhang(张靖仪), Tangmei He(何唐梅)
Chin. Phys. B, 2018, 27 (**3**): 030401. DOI: 10.1088/1674-1056/27/3/030401

A note on the mass of Kerr-AdS black holes in the off-shell generalized ADT formalism

Yi-De Jing(景艺德), Jun-Jin Peng(彭俊金)
Chin. Phys. B, 2017, 26 (**10**): 100401. DOI: 10.1088/1674-1056/26/10/100401

Solution of Dirac equation around a charged rotating black hole

Lü Yan (吕嫣), Hua Wei (花巍)
Chin. Phys. B, 2014, 23 (**4**): 040403. DOI: 10.1088/1674-1056/23/4/040403

The stability of a shearing viscous star with an electromagnetic field

M. Sharif, M. Azama
Chin. Phys. B, 2013, 22 (**5**): 050401. DOI: 10.1088/1674-1056/22/5/050401

RAPID COMMUNICATION

Model on picometer-level light gravitational delay in the GRACE Follow-On-like missions

Jin-Zhuang Dong(董金壮), Wei-Sheng Huang(黄玮圣), Cheng-Gang Qin(秦成刚)[†], Yu-Jie Tan(谈玉杰)[‡], and Cheng-Gang Shao(邵成刚)[§]

MOE Key Laboratory of Fundamental Physical Quantities Measurement & Hubei Key Laboratory of Gravitation and Quantum Physics, PGMF and School of Physics, Huazhong University of Science and Technology, Wuhan 430074, *China*

(Received 20 June 2024; revised manuscript received 14 August 2024; accepted manuscript online 14 September 2024)

Laser interferometry plays a crucial role in laser ranging for high-precision space missions such as GRACE (Gravity Recovery and Climate Experiment) Follow-On-like missions and gravitational wave detectors. For such accuracy of modern space missions, a precise relativistic model of light propagation is required. With the post-Newtonian approximation, we utilize the Synge world function method to study the light propagation in the Earth's gravitational field, deriving the gravitational delays up to order c^{-4}. Then, we investigate the influences of gravitational delays in three inter-satellite laser ranging techniques, including one-way ranging, dual one-way ranging, and transponder-based ranging. By combining the parameters of Kepler orbit, the gravitational delays are expanded up to the order of e^2 (e is the orbital eccentricity). Finally, considering the GRACE Follow-On-like missions, we estimate the gravitational delays to the level of picometer. The results demonstrate some high-order gravitational and coupling effects, such as c^{-4}-order gravitational delays and coupling of Shapiro and beat frequency, which may be non-negligible for higher precision laser ranging in the future.

Keywords: classical general relativity, post-Newtonian approximation, phase shifting interferometry

PACS: 04.20.–q, 04.25.Nx, 42.87.Bg **DOI:** 10.1088/1674-1056/ad7af9

1. Introduction

The Gravity Recovery and Climate Experiment (GRACE) satellites are a very successful space mission. It uses a high-precision microwave ranging system to measure temporal distance variations between the two satellites and then to map the Earth's gravitational field. The GRACE Follow-On (GRACE-FO) is a continuation of the mission on near-identical hardware, launched in May 2018. GRACE-FO is equipped with the novel laser ranging interferometer (LRI), a technology demonstrator for proving the feasibility of laser interferometry for inter-satellite ranging measurements. The LRI measurement is performed by interfering the laser on the local satellite with the received laser signal transmitted by the far satellite, and then tracking the phase of the resulting beatnote. It provides the inter-satellite ranging measurements with a precision up to 1 nm/Hz$^{1/2}$ in frequencies above 100 mHz.[1] The successful commissioning of the LRI was an essential step towards the Laser Interferometer Space Antenna (LISA) mission,[2] which will use comparable inter-satellite laser ranging technology between three spacecrafts in deep space for the detection of gravitational waves. In addition, LRI will demonstrate precision inter-spacecraft laser interferometry for future GRACE-FO-like missions. For these space missions, it is necessary to develop a precise relativistic model for light propagation in the Earth's gravitational field. In recent years, the LRI has undergone notable advancements, enabling the attainment of pm/$\sqrt{\text{Hz}}$ scale in the ranging measurements. LRI of this precision will be equipped in future high-precision space missions to conduct scientific exploration or test fundamental physics.[3] In those missions, it is important to consider the gravitational effects to the pm scale.

The core concept of general relativity is that the presence of energy results in the bending effect of space–time, where objects move along their geodesic in curved space–time.[4] In contrast to Newton frame where light propagates in straight lines, general relativity dictates that light follows its geodesic, leading to the bending of light trajectories in the presence of massive objects.[5] This bending of light trajectories is of significant importance in gravitational physics. Light signal in the curved space–time can serve as highly effective tools to explore crucial information about the nature of space–time, such as measuring the post-Newtonian parameter[6,7] and testing the Lorentz symmetry.[8–10] It is widely applied in high-precision experiments and measurements, enabling scientists to gain a deeper understanding of the gravitational effects caused by massive objects.[11–14]

In the framework of general relativity, the light propagation is determined by the standard method of solving null geodesic equation. Based on null geodesic equation, the light propagation has been studied in the case of static spheri-

[†]Corresponding author. E-mail: cgqin@hust.edu.cn
[‡]Corresponding author. E-mail: yjtan@hust.edu.cn
[§]Corresponding author. E-mail: cgshao@hust.edu.cn

© 2024 Chinese Physical Society and IOP Publishing Ltd

cally symmetric space–time,[15,16] and Kerr–Newman space–time,[17–19] the space–times of rotating stratified ellipsoids,[20] etc. And Refs. [21–23] conducted an in-depth analysis of the light propagation up to 1PN, 1.5PN, and 2PN in the gravitational field of N arbitrarily moving extended bodies. In addition, based on the world function or time transfer function, many solutions have been proposed for the light propagation in the post-Newtonian and post-Minkowskian approximations.[24–33] These solutions of light propagation can be applied to space missions to analyze relativistic effects.

In this paper, we use the method of Synge world function to study the influences of gravitational delay for the GRACE-FO-like missions. The theoretical model is then integrated with the actual light path of LRI to analyze the impact of gravitational delays. The Kepler orbit model is utilized to evaluate the magnitude of each gravitational effect term. Considering GRACE-FO concept and parameters, the influences of gravitational delay are estimated to the level of pm. The organization of this paper is as follows. In Section 2, we provide a brief introduction to the world function and its expression to c^{-4} order. We then use the world function to derive the expression of the time delay function up to c^{-5} order. In Section 3, we discuss the specific expression of the time delay function in the Earth's gravitational field. In Section 4, space–time diagrams are employed to model three types of laser rangings: one-way ranging, dual one-way ranging, and transponder-based ranging. Furthermore, an analysis is conducted to examine the impact of the time delay function on ranging. In Section 5, we evaluate the magnitude of each effect of the gravitational delay based on GRACE-FO-like missions and analyze the items that may reach the magnitude of pm. Finally, in Section 6, we present the conclusion and outlook.

In this paper, the Newton gravitational constant is given by G, and the speed of light in vacuum is represented by c. The Lorentzian metric of space–time is denoted by g, and the signature adopted for $g_{\mu\nu}$ is $(+---)$. We assume that the space–time is covered by a global coordinate system $(x^\mu) = \left(x^0 = ct, x^1, x^2, x^3\right)$. We suppose that the curves of equations $x^i = \text{const.}$ are timelike, meaning $g_{00} > 0$ anywhere. $\boldsymbol{a}\cdot\boldsymbol{b}$ is denoted by $a_i b^i$ and Einstein's repeated index convention is adopted here. For function $f(x^\rho)$, $f_{,\rho} = \partial f/\partial x^\rho$ means the partial derivative of the function with respect to the coordinates x^ρ.

2. World function and time delay function

2.1. Definition of world function

The space–time background can be considered a well-structured sub-manifold within the universe. Given a point A on this manifold, there exists a convex neighborhood O that contains A. Any point B within O has a unique differential curve that connects it to A. This differentiable curve is also called a geodesic. The geodesic can be defined by parameters $x^\mu = x^\mu(\zeta)$, where $\zeta \in \mathbb{R}$ and $\zeta_A \le \zeta \le \zeta_B$. For above two points A and B, the world function can be expressed as[4]

$$\Omega(x_A, x_B) = \frac{1}{2}\int_{\zeta_A}^{\zeta_B} g_{\mu\nu}(x^\alpha(\lambda))\frac{\mathrm{d}x^\mu}{\mathrm{d}\lambda}\frac{\mathrm{d}x^\nu}{\mathrm{d}\lambda}\mathrm{d}\lambda, \tag{1}$$

where λ is the affine parameter. For the case where A and B are connected by a null geodesic,

$$\Omega(x_A, x_B) = 0. \tag{2}$$

Here, $\Omega(x_A, x) = 0$ represents the light cone of A. Solving the light cone equation for x_A yields two distinct solutions x^+ and x^-, as the light-like curve equation $\Omega(x_A, x) = 0$ intersects the light cone at two points in the future and in the past. We assume that A denotes the point at which the light signal is emitted, and B corresponds to the point at which it is received. The corresponding travel time is characterized as

$$(x_B^{0+} - x_A^0) = c\mathcal{T}_e(t_A, \boldsymbol{x}_A, \boldsymbol{x}_B), \tag{3}$$

where $\mathcal{T}_e(t_A, \boldsymbol{x}_A, \boldsymbol{x}_B)$ is the time transfer function.

2.2. Time delay function for weak field approximation to $1/c^4$

For a weak-field gravitational field, the space–time metric can be regarded as a flat space–time metric plus a gravitational perturbation. The space–time metric can be expanded by a series in ascending powers of G[4]

$$g_{\mu\nu} = \eta_{\mu\nu} + \sum_n g_{\mu\nu}^{(n)}, \tag{4}$$

where $g_{\mu\nu}^{(n)} = g_{\mu\nu}^{(n)}(G^n)$. According to the property of the metric component $g_{\mu\rho}g^{\rho\nu} = \delta_\mu^\nu$, one has

$$\begin{cases} g_{(1)}^{\mu\nu} = -\eta^{\mu\rho}\eta^{\nu\sigma}g_{\rho\sigma}^{(1)}, \\ g_{(n)}^{\mu\nu} = -\eta^{\mu\rho}\eta^{\nu\sigma}g_{\rho\sigma}^{(n)} - \sum\limits_{p=1}^{n-1}\eta^{\mu\rho}g_{\rho\sigma}^{(p)}g_{(n-p)}^{\nu\sigma}. \end{cases} \tag{5}$$

Substituting Eq. (4) into Eq. (1), the world function can be written as

$$\Omega(x_A, x_B) = \Omega^{(0)}(x_A, x_B) + \sum_{n=1}^{\infty}\Omega^{(n)}(x_A, x_B), \tag{6}$$

where $\Omega^{(0)}$ corresponds to the flat space–time, and $\Omega^{(n)}$ represents the perturbation term of G^n. For flat space–time, the Newton order light-trajectory equation is defined as

$$x_{(0)}^\alpha(\lambda) = (x_B^\alpha - x_A^\alpha)\lambda + x_A^\alpha, \qquad 0 \le \lambda \le 1. \tag{7}$$

Substituting Eq. (7) into Eq. (1), the 0-th order expression of the world function can be obtained by integrating along the Newtonian light path

$$\Omega^{(0)}(x_A, x_B) = \frac{1}{2}\eta_{\mu\nu}\left(x_B^\mu - x_A^\mu\right)\left(x_B^\nu - x_A^\mu\right). \tag{8}$$

Under the condition of weak field approximation, the n-th perturbation $\Omega^{(n)}$ can be also calculated along the Newtonian light path[4]

$$\Omega^{(1)}(x_A,x_B)=\frac{1}{2}\left(x_B^\mu-x_A^\mu\right)\left(x_B^\nu-x_A^\nu\right)\times\int_0^1 g_{\mu\nu}^{(1)}\left(x_{(0)}(\lambda)\right)\mathrm{d}\lambda, \tag{9}$$

$$\Omega^{(1.5)}(x_A,x_B)=\frac{1}{2}\left(x_B^\mu-x_A^\mu\right)\left(x_B^\nu-x_A^\nu\right)\times\int_0^1 g_{\mu\nu}^{(1.5)}\left(x_{(0)}(\lambda)\right)\mathrm{d}\lambda, \tag{10}$$

$$\begin{aligned}\Omega^{(2)}(x_A,x_B)=&\frac{1}{2}(x_B^\mu-x_A^\mu)(x_B^\nu-x_A^\nu)\int_0^1\Big[g_{\mu\nu}^{(2)}(x_{(0)}(\lambda))\\&-\eta^{\rho\sigma}g_{\mu\rho}^{(1)}(x_{(0)}(\lambda))g_{\nu\sigma}^{(1)}(x_{(0)}(\lambda))\\&-\eta^{\rho\sigma}\frac{\partial\Omega^{(1)}}{\partial x^\rho}(x_A,x_{(0)}(\lambda))\frac{\partial g_{\mu\nu}^{(1)}}{\partial x^\sigma}(x_{(0)}(\lambda))\Big]\mathrm{d}\lambda\\&+\frac{1}{2}\eta^{\mu\nu}\frac{\partial\Omega^{(1)}}{\partial x_B^\mu}(x_A,x_B)\frac{\partial\Omega^{(1)}}{\partial x_B^\nu}(x_A,x_B).\end{aligned} \tag{11}$$

The relationship between the time transfer functions and the world function is as follows:

$$\mathcal{T}_e^{(1)}=-\frac{\tilde{\Omega}_e^{(1)}}{c\left|\boldsymbol{x}_B-\boldsymbol{x}_A\right|}, \tag{12}$$

$$\mathcal{T}_e^{(1.5)}=-\frac{\tilde{\Omega}_e^{(1.5)}}{c\left|\boldsymbol{x}_B-\boldsymbol{x}_A\right|}, \tag{13}$$

$$\mathcal{T}_e^{(2)}=-\frac{1}{cR_{AB}}[\tilde{\Omega}_e^{(2)}+c\mathcal{T}_e^{(1)}\tilde{\Omega}_{e|1}^{(1)}+\frac{1}{2}c^2(\mathcal{T}_e^{(1)})^2], \tag{14}$$

where $\tilde{\Omega}_{e|k}^{(n)}(t_A,\boldsymbol{x}_A,\boldsymbol{x}_B)=\partial^k\Omega^{(n)}/\left(\partial x_B^0\right)^k$.

3. The time delay function in the Earth's gravitational field

The covariant nature of Einstein's theory ensures that physical measurements remain independent of the choice of coordinate system. It is essential to select an appropriate coordinate system with definite properties. The geocentric celestial reference system (GCRS) with the center of mass of the Earth as the origin of coordinates is suitable for studying the gravitational effects in the vicinity of the Earth. The GCRS is defined with the coordinates $x^\mu\equiv(ct,x^i)$, with t the geocentric coordinate time. As IAU Resolution B1.3 (2000),[34] the metric tensor of the GCRS can be expressed in the form of scalar potential and vector potential

$$\begin{cases}g_{00}=1-\frac{2}{c^2}W+\frac{2\beta}{c^4}W^2,\\ g_{0i}=\frac{2(\gamma+1)}{c^3}W_i,\\ g_{ij}=-\delta_{ij}\left(1+\frac{2\gamma}{c^2}W+\frac{3\delta}{2c^4}W^2\right),\end{cases} \tag{15}$$

where β and γ are the usual post-Newtonian parameters, and δ is the post-post-Newtonian parameters (in general relativity $\beta=\gamma=\delta=1$). The expression of scalar potential W and vector potential $\boldsymbol{W}$ (the Earth's spin axis is set as z-axis) is given by[35]

$$W(\boldsymbol{x})=GM\left[\frac{1}{r}-\sum_{n=2}^{\infty}\frac{1}{n!}J_nR_{\mathrm{E}}^n\frac{\partial^n}{\partial z^n}\left[\frac{1}{r}\right]\right], \tag{16}$$

$$W_i(\boldsymbol{x})=-\frac{1}{2}GM\varepsilon_{ijk}S^j\partial^k\left[\frac{1}{r}-\sum_{n=1}^{\infty}\frac{1}{n!}K_nR_{\mathrm{E}}^n\frac{\partial^n}{\partial z^n}\left(\frac{1}{r}\right)\right], \tag{17}$$

where K_n is the relativistic coefficients, and J_n is the Newtonian multipole moments. Suppose that the spatial part of the geodesic connecting x_A and x_B lies entirely outside the Earth. Substituting Eq. (15) into Eqs. (9)–(11), the world function becomes

$$\Omega^{(1)}(x_A,x_B)=-\frac{1}{c^2}\left[\left(x_B^0-x_A^0\right)^2+\gamma R_{AB}^2\right]\int_0^1 W\,\mathrm{d}\lambda, \tag{18}$$

$$\Omega^{(1.5)}(x_B,x_A)=\frac{2(\gamma+1)}{c^3}\left(x_B^0-x_A^0\right)\left(x_B^i-x_A^i\right)\int_0^1 W_i\mathrm{d}\lambda, \tag{19}$$

$$\begin{aligned}\Omega^{(2)}(x_A,x_B)=&\frac{1}{4c^4}\Big[(4\beta-8)\left(x_B^0-x_A^0\right)^2\\&+\left(8\gamma^2-3\delta\right)R_{AB}^2\Big]\int_0^1 W^2\mathrm{d}\lambda\\&-\frac{1}{c^2}\left[\left(x_B^0-x_A^0\right)^2+\gamma R_{AB}^2\right]\\&\times\int_0^1\delta^{ij}\frac{\partial\Omega^{(1)}}{\partial x^i}\frac{\partial W}{\partial x^j}\mathrm{d}\lambda\\&+\frac{1}{2}\eta^{\mu\nu}\frac{\partial\Omega^{(1)}}{\partial x_B^\mu}(x_A,x_B)\frac{\partial\Omega^{(1)}}{\partial x_B^\nu}(x_A,x_B).\end{aligned} \tag{20}$$

The world functions can be transformed into the integral of the scalar potential and the vector potential. For simplicity, we can introduce differential operators for the kernel function to express the integral of the scalar potential and the vector potential. To calculate the integral of the gravitational potentials, we define the kernel function, which is represented as

$$\begin{aligned}F(\boldsymbol{x},\boldsymbol{x}_A,\boldsymbol{x}_B)=&\int_0^1\frac{1}{r}\mathrm{d}\lambda\\=&\int_0^1\frac{1}{\left(x_B^\alpha-x_A^\alpha\right)\lambda+x_A^\alpha}\mathrm{d}\lambda\\=&\frac{1}{R_{AB}}\ln\left(\frac{\rho_+}{\rho_-}\right)_{|\boldsymbol{x}=0},\end{aligned} \tag{21}$$

$$F(\boldsymbol{x},\boldsymbol{x}_A,\boldsymbol{x}_B)=\frac{1}{R_{AB}}\ln\left(\frac{|\boldsymbol{x}-\boldsymbol{x}_B|+|\boldsymbol{x}-\boldsymbol{x}_B|+R_{AB}}{|\boldsymbol{x}-\boldsymbol{x}_B|+|\boldsymbol{x}-\boldsymbol{x}_B|-R_{AB}}\right), \tag{22}$$

$$\begin{aligned}\frac{\partial F}{\partial x_B^i}=&-\frac{R_{AB,i}}{R_{AB}^3}\ln\left(\frac{r_A+r_B+R_{AB}}{r_A+r_B-R_{AB}}\right)\\&-\frac{x_{B,i}}{r_Ar_B^2(1+\boldsymbol{n}_A\cdot\boldsymbol{n}_B)}\\&+\frac{r_A+r_B}{r_Ar_B(1+\boldsymbol{n}_A\cdot\boldsymbol{n}_B)}\frac{R_{AB,i}}{R_{AB}^2},\end{aligned} \tag{23}$$

where $\rho_\pm=|\boldsymbol{x}-\boldsymbol{x}_A|+|\boldsymbol{x}-\boldsymbol{x}_B|\pm R_{AB}$ and $R_{AB}=|\boldsymbol{x}_B-\boldsymbol{x}_A|$ represent the Euclidean norms of $\boldsymbol{x}_A$ and $\boldsymbol{x}_B$. Then the integral

of the gravitational potential can be rewritten as the differential operators acting on the kernel function

$$\int_0^1 W\,\mathrm{d}\lambda = GM\left[1-\sum_{n=2}^{\infty}\frac{1}{n!}J_n R_{\mathrm{E}}^n\frac{\partial^n}{\partial z^n}\right]F, \tag{24}$$

$$\int_0^1 W_i\,\mathrm{d}\lambda = -\frac{1}{2}G\epsilon_{ijk}S^j\partial^k\left[1-\sum_{n=1}^{\infty}\frac{1}{n!}K_n R_{\mathrm{E}}^n\frac{\partial^n}{\partial z^n}\right]F, \tag{25}$$

where $\boldsymbol{S}=I\boldsymbol{e}_z$ is the moment of inertia of the Earth. By substituting Eqs. (24)–(25) into Eqs. (18)–(20), the expressions of the world function can be obtained. To describe the influences of mass multipole moments, we define the quantity as

$$T_{A_n}(\boldsymbol{x}_A,\boldsymbol{x}_B) = \frac{1}{n!}A_n R_{\mathrm{E}}^n\frac{\partial^n}{(\partial x^3)^n}F, \tag{26}$$

where we introduce the coefficient A_{2n} to represent J_{2n} or K_{2n} to increase the concision of the following expressions. In Eq. (26), we have used the following abbreviations:

$$\begin{aligned}T_{A_n}(\boldsymbol{x},\boldsymbol{x}_A,\boldsymbol{x}_B) &= \frac{1}{R_{AB}}A_n R_{\mathrm{E}}^n\sum_{m=1}^{n}\left[\frac{1}{{\rho_-}^{n-m+1}}-\frac{1}{{\rho_+}^{n-m+1}}\right]\\ &\quad\times\Theta_{nm}(\boldsymbol{x},\boldsymbol{x}_A,\boldsymbol{x}_B),\end{aligned} \tag{27}$$

where

$$\begin{aligned}\Theta_{nm}(\boldsymbol{x},\boldsymbol{x}_A,\boldsymbol{x}_B) &= (-1)^{n-m}\\ &\quad\times\sum_{i_1,\cdots,i_m}\left(\frac{(n-m)!}{i_1!i_2!\cdots i_m!}\prod_{l=1}^{m}\left[S_l(\boldsymbol{x},\boldsymbol{x}_A,\boldsymbol{x}_B)\right]^{i_l}\right),\end{aligned} \tag{28}$$

$$\begin{aligned}S_l(\boldsymbol{x},\boldsymbol{x}_A,\boldsymbol{x}_B) &= \frac{1}{|\boldsymbol{x}-\boldsymbol{x}_A|^{l-1}}C_l^{(-1/2)}(\kappa_A)\\ &\quad+\frac{1}{|\boldsymbol{x}-\boldsymbol{x}_B|^{l-1}}C_l^{(-1/2)}(\kappa_B),\end{aligned} \tag{29}$$

where $C_l^{(-1/2)}$ is the Gegenbauer polynomial of degree l, and $\kappa_{A/B}=\frac{\boldsymbol{k}\cdot(\boldsymbol{x}-\boldsymbol{x}_{A/B})}{|\boldsymbol{x}-\boldsymbol{x}_{A/B}|}$. The summation sign of the above formula satisfies the following formula:

$$\begin{cases} i_1+2i_2+3i_3+\cdots+mi_m=n,\\ i_1+i_2+\cdots+i_m=n-m+1.\end{cases} \tag{30}$$

To calculate the 2rd world function of Eq. (20), the first term (the integral term of the gravitational-potential square) can be calculated as

$$\int_0^1 W^2\,\mathrm{d}\lambda = G^2M^2\int_0^1\frac{1}{r^2}\,\mathrm{d}\lambda, \tag{31}$$

where due to the limitation of the accuracy of space missions, the high-order terms of spherical harmonic coefficients in gravitational potential are neglected (this approximation will be discussed later in the numerical analysis). Similarly one can define the quadratic kernel function

$$\Phi(x_A,x_B) = \int_0^1\frac{1}{r^2}\,\mathrm{d}\lambda = \frac{\arccos(\boldsymbol{n}_A\cdot\boldsymbol{n}_B)}{r_A r_B\sqrt{1-(\boldsymbol{n}_A\cdot\boldsymbol{n}_B)^2}}. \tag{32}$$

Then, the second term of Eq. (20) can be calculated by further mathematical procedure

$$\begin{aligned}&-\frac{1}{c^2}\left[\left(x_B^0-x_A^0\right)^2+\gamma R_{AB}^2\right]\int_0^1\delta^{ij}\frac{\partial\Omega^{(1)}}{\partial x^i}\frac{\partial W}{\partial x^j}\,\mathrm{d}\lambda\\ &=\frac{G^2M^2}{c^4}\left[\left(x_B^0-x_A^0\right)^2+\gamma R_{AB}^2\right]\\ &\quad\times\left[\left(1+\frac{r_A}{r_B}\right)\frac{1}{R_{AB}^2}\frac{\left(x_B^0-x_A^0\right)^2+\gamma R_{AB}^2}{r_A r_B+(\boldsymbol{x}_A\cdot\boldsymbol{x}_B)}\right.\\ &\quad\left.-\frac{\left(x_B^0-x_A^0\right)^2-\gamma R_{AB}^2}{R_{AB}^2}\frac{F(x_A,x_B)}{r_B}-2\gamma\Phi\right].\end{aligned} \tag{33}$$

The third term of Eq. (20) does not involve integration and can be calculated directly.

In conclusion, the total time delay contribution can be expressed as follows:

$$\begin{aligned}\mathcal{T}_e &\equiv \mathcal{T}_e^{(\mathrm{Shapiro})}+\mathcal{T}_e^{(J_2)}+\mathcal{T}_e^{(J_3)}+\mathcal{T}_e^{(J_4)}\\ &\quad+\mathcal{T}_e^{(S)}+\mathcal{T}_e^{(K_1)}+\mathcal{T}_e^{(G^2)},\end{aligned} \tag{34}$$

where the first term is the well-known Shapiro time delay, the second, third and fourth terms represent the contribution of mass multipole moments, the fifth and sixth terms indicate the contribution of the rotation of the Earth, and the seventh term is the contribution of G^2, and their expressions are given by

$$\mathcal{T}_e^{(\mathrm{Shapiro})} = \frac{GM(1+\gamma)R_{AB}}{c^3}\ln\left(\frac{\widehat{\rho}_+}{\widehat{\rho}_-}\right), \tag{35}$$

$$\begin{aligned}\mathcal{T}_e^{(J_2)} &= \frac{GM(1+\gamma)J_2R_{\mathrm{E}}^2}{2c^3}\left\{\left[\frac{1}{(\widehat{\rho}_-)^2}-\frac{1}{(\widehat{\rho}_+)^2}\right][\widehat{\kappa}_A+\widehat{\kappa}_B]\right.\\ &\quad\left.-\left(\frac{1}{\widehat{\rho}_-}-\frac{1}{\widehat{\rho}_+}\right)\left[\frac{\left(1-(\widehat{\kappa}_A)^2\right)}{r_A}+\frac{\left(1-(\widehat{\kappa}_B)^2\right)}{r_B}\right]\right\},\end{aligned} \tag{36}$$

$$\begin{aligned}\mathcal{T}_e^{(J_3)} &= (-1)\frac{GM(1+\gamma)}{c^3}J_3R_{\mathrm{E}}^3\left\{\left(\frac{1}{\widehat{\rho}_-^3}-\frac{1}{\widehat{\rho}_+^3}\right)\frac{(-1)}{3}(\widehat{\kappa}_A+\widehat{\kappa}_B)^3\right.\\ &\quad+\left(\frac{1}{\widehat{\rho}_-^2}-\frac{1}{\widehat{\rho}_+^2}\right)(-1)(\widehat{\kappa}_A+\widehat{\kappa}_B)\left(\frac{1}{r_A}\left[\frac{1}{2}(1-\widehat{\kappa}_A^2)\right]\right.\\ &\quad\left.+\frac{1}{r_B}\left[\frac{1}{2}(1-\widehat{\kappa}_B^2)\right]\right)+\left(\frac{1}{\widehat{\rho}_-}-\frac{1}{\widehat{\rho}_+}\right)\\ &\quad\left.\times\left(\frac{1}{r_A^2}\frac{\widehat{\kappa}_A}{2}(1-\widehat{\kappa}_A^2)+\frac{1}{r_B^2}\frac{\widehat{\kappa}_B}{2}(1-\widehat{\kappa}_B^2)\right)\right\},\end{aligned} \tag{37}$$

$$\begin{aligned}\mathcal{T}_e^{(J_4)} &= (-1)\frac{GM(1+\gamma)}{c^3}J_4R_{\mathrm{E}}^4\left\{\left(\frac{1}{\widehat{\rho}_-^4}-\frac{1}{\widehat{\rho}_+^4}\right)\frac{(-1)}{4}(\widehat{\kappa}_A+\widehat{\kappa}_B)^4\right.\\ &\quad+\left(\frac{1}{\widehat{\rho}_-^3}-\frac{1}{\widehat{\rho}_+^3}\right)(\widehat{\kappa}_A+\widehat{\kappa}_B)^2\left(\frac{1}{r_A}\left[\frac{1}{2}\left(1-\widehat{\kappa}_A^2\right)\right]\right.\\ &\quad\left.\left.+\frac{1}{r_B}\left[\frac{1}{2}\left(1-\widehat{\kappa}_B^2\right)\right]\right)\right]+\left(\frac{1}{\widehat{\rho}_-^2}-\frac{1}{\widehat{\rho}_+^2}\right)(-1)\end{aligned}$$

$$\times\left[\frac{1}{2}\left(\frac{1}{r_A}\left[\frac{1}{2}(1-\widehat{\kappa}_A^2)\right]+\frac{1}{r_B}\left[\frac{1}{2}(1-\widehat{\kappa}_B^2)\right]\right)^2 -(\widehat{\kappa}_A+\widehat{\kappa}_B)\left(\frac{1}{r_A^2}\frac{\widehat{\kappa}_A}{2}(1-\widehat{\kappa}_A^2)+\frac{1}{r_B^2}\frac{\widehat{\kappa}_B}{2}(1-\widehat{\kappa}_B^2)\right)\right] +\left(\frac{1}{\widehat{\rho}_-}-\frac{1}{\widehat{\rho}_+}\right)\left[\frac{1}{r_A^3}\left(\frac{1}{4}\right)\left[\frac{5\widehat{\kappa}_A^2}{2}(1-\widehat{\kappa}_A^2)-\frac{1}{2}(1-\widehat{\kappa}_A^2)\right] +\frac{1}{r_B^3}\left(\frac{1}{4}\right)\left[\frac{5\widehat{\kappa}_B^2}{2}(1-\widehat{\kappa}_B^2)-\frac{1}{2}(1-\widehat{\kappa}_B^2)\right]\right]\Bigg\}, \tag{38}$$

$$\mathcal{T}_e^{(S)}=\frac{GM(\gamma+1)}{c^4}\left(\frac{1}{r_A}+\frac{1}{r_B}\right)\frac{(\boldsymbol{n}_A\times\boldsymbol{n}_B)\cdot\boldsymbol{S}}{(1+\boldsymbol{n}_A\cdot\boldsymbol{n}_B)}, \tag{39}$$

$$\begin{aligned}\mathcal{T}_e^{(K_1)} =& \frac{GM(\gamma+1)K_1R_{\rm E}\boldsymbol{S}}{R_{AB}c^4}\cdot\Bigg\{\left[\frac{1}{(\widehat{\rho}_+)^2}-\frac{1}{(\widehat{\rho}_-)^2}\right]\\ &\times[(\boldsymbol{n}_A+\boldsymbol{n}_B)\times\boldsymbol{R}_{AB}](\widehat{\kappa}_A+\widehat{\kappa}_B)\\ &+\left[\frac{1}{\widehat{\rho}_+}-\frac{1}{\widehat{\rho}_-}\right]\left[(\boldsymbol{R}_{AB}\times\boldsymbol{k})\left(\frac{1}{r_A}+\frac{1}{r_B}\right)\right.\\ &\left.-\frac{\widehat{\kappa}_A(\boldsymbol{R}_{AB}\times\boldsymbol{n}_A)}{r_A}-\frac{\widehat{\kappa}_B(\boldsymbol{R}_{AB}\times\boldsymbol{n}_B)}{r_B}\right]\Bigg\},\end{aligned} \tag{40}$$

$$\begin{aligned}\mathcal{T}_e^{(G^2)} =& -\frac{G^2M^2R_{AB}}{4c^5}[4\beta-8-8\gamma-3\epsilon]\\ &\times\frac{\arccos(\boldsymbol{n}_A\cdot\boldsymbol{n}_B)}{r_Ar_B\sqrt{1-(\boldsymbol{n}_A\cdot\boldsymbol{n}_B)^2}}\\ &+\frac{G^2M^2R_{AB}}{c^5}\left[\frac{(1+\gamma)^2}{r_Ar_B(1+\boldsymbol{n}_A\cdot\boldsymbol{n}_B)}\right].\end{aligned} \tag{41}$$

4. Modeling of the inter-satellite ranging

Using the analysis of the ranging principle presented in Ref. [36], we extend the analysis of relativistic time delay on the original basis. The LRI measures the interference of light signals, and its essence is the phase difference of light. The phase of light can provide all the information about light propagation in the gravitational field. Inter-satellite ranging involves measuring distance changes between satellites by exchanging laser signals. $\rho(t)$ is defined as the instantaneous distance between two satellites

$$\rho(t)=\rho_{\rm inst}(t)=|\boldsymbol{r}_1(t)-\boldsymbol{r}_2(t)|, \tag{42}$$

where the space vectors $\boldsymbol{r}_1$ and $\boldsymbol{r}_2$ are defined in the quasi-inertial non-rotating system GCRS. In the following content, we discuss three ranging models, namely, one-way ranging, dual one-way ranging, and transponder-based ranging, and derive their respective phase expressions.

4.1. One-way ranging

The space–time diagram of one-way ranging optical path is shown in Fig. 1. The satellite S/C i sends a light signal at the moment E. After transmitting in free space, this light signal is received by satellite S/C j at moment C, and then interferes with the local signal at the moment A. Therefore, the output of the phasemeter on the satellite S/C j is

$$\begin{aligned}\varphi_{{\rm PM}|j}(t_A) &= \left|\Phi_{in,j}(\tau_j(t_A))\right|\\ &= \left|\Phi_{i|j}(\tau_j(t_A))-\Phi_{j|j}(\tau_j(t_A))\right|\\ &= \pm\left(\Phi_{i|j}(\tau_j(t_A))-\Phi_{j|j}(\tau_j(t_A))\right),\end{aligned} \tag{43}$$

where t_A is the coordinate time of the phasemeter in GCRS. The symbol Φ represents the measured value obtained from the phase meter, and the subscript $|l$ $(l=i,j)$ indicates the physical quantity observed in the co-moving system of $|l$. The transmitting satellite is denoted by S/C i, and the receiving satellite by S/C j. The output $\varphi_{{\rm PM}|j}(t_A)$ is measured in the co-moving coordinate system of S/C j, where "+" indicates that the received signal laser phase is higher than the local laser phase (i.e., $\Phi_{i|j}(\tau_j(t_A))>\Phi_{j|j}(\tau_j(t_A))$). The local laser phase emitted by S/C j is expressed in its co-moving coordinate system as $\Phi_{j|j}(B)=\bar{\omega}_{j|j}\cdot\tau_j(t_B)$. As the world line of light is a constant phase line, the signal phases of the transmitting and receiving space–time points are equal. Therefore, the phase expression of the local laser signal of S/C j in its co-moving coordinate system can be obtained as

$$\begin{aligned}\Phi_{j|j}(\tau_j(t_A)) &= \Phi_{j|j}(A)=\Phi_{j|j}(\tau_j(t_B))=\Phi_{j|j}(B)\\ &= \bar{\omega}_{j|j}\cdot\tau_j(t_A-\Delta t_{BA}),\end{aligned} \tag{44}$$

where Δt_{BA} is the difference between the coordinates of two space–time points. To convert the optical signal from S/C i to S/C j, the phase of light is transformed from the co-moving system of S/C i to S/C j using the Lorentz invariant property of light phase $\Phi_{i|j}(A)=\Phi_{i|i}(A)$ based on the relationship between phase and angular frequency

$$\begin{aligned}\Phi_{i|j}(\tau_j(t_A)) &= \int^{\tau_j(t_A)}\omega_{i|j}(\tau_j)\,{\rm d}\tau_j+{\rm const.}\\ &= \bar{\omega}_{i|i}\cdot\tau_i(t_A-\Delta t_{EA}).\end{aligned} \tag{45}$$

Then with this relation, the output of the phasemeter receiving S/C j can be rewritten as

$$\begin{aligned}\varphi_{{\rm PM}|j}(t) =& \pm\bar{\omega}_{i|i}\cdot\tau_i(t_A-\Delta t_{EA})\mp\bar{\omega}_{j|j}\cdot\tau_j(t_A-\Delta t_{BA})\\ &+{\rm const.},\end{aligned} \tag{46}$$

where the travel time of photons between events, denoted by Δt, incorporates the relativistic effects.

Let us introduce the variable $\delta\tau(t)\equiv t-\tau(t)$, where τ is the proper time of a satellite. From the general relativity, the relation between proper time and coordinate time is given by

$$\tau(t)=\frac{1}{c}\int\sqrt{c^2g_{00}+2cg_{0i}v^i+g_{ij}v^iv^j}\,{\rm d}t, \tag{47}$$

where $v = \mathrm{d}x^i/\mathrm{d}t$ is the coordinate velocity. In the weak gravitational field approximation, the proper time of the satellite can be expressed as

$$\tau(t) = t\left(1 - \frac{v^2}{2c^2} - \frac{W}{c^2} - \frac{\gamma W v^2}{c^4} + \frac{2(\gamma+1)}{c^3}\boldsymbol{W}\cdot\frac{\boldsymbol{v}}{c} + \frac{\beta W^2}{c^4}\right) + \mathrm{O}\left(c^{-5}\right). \tag{48}$$

It can be estimated $\delta\dot{\tau}(t) \sim GM/(R_{\mathrm{E}}c^2) \sim 10^{-10}$.

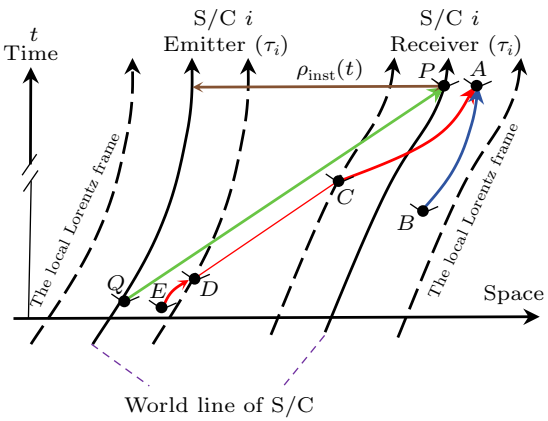


Fig. 1. The space–time diagram of the optical path of one-way ranging. (i) E event represents the space–time point of the optical signal emitted by S/C i; D event represents the space–time point when the laser signal flies out of S/C i and enters the vacuum environment; C event represents the space–time point when the transmitted laser signal enters S/C j; B event represents the space–time point when the local laser signal is emitted by S/C j; A event represents the interference between the transmitted signal of S/C i and the local optical signal of S/C j. (ii) The red part and dark blue part are the actual light path, and the green part is the ideal light path. (iii) Because the complex structure inside the satellite has a relativistic deflection effect on the light path, the light path in the ED segment and the BA segment is not a quasi-slanted straight line. The DC segment is the propagation of light in a vacuum, which is considered as an ideal situation.

To develop the output of the phasemeter, Eq. (46), we introduce two quantities of light angular frequency

$$\begin{cases} \tilde{\omega} = \frac{\bar{\omega}_{i|i} + \bar{\omega}_{j|j}}{2}, \\ \Delta\tilde{\omega} = \left|\bar{\omega}_{i|i} - \bar{\omega}_{j|j}\right|. \end{cases} \tag{49}$$

Then substituting Eq. (49) into Eq. (46), the output of the phasemeter can be reexpressed as

$$\begin{aligned} \varphi_{\mathrm{PM}|j}(t) = {} & \Delta\tilde{\omega}t \mp \tilde{\omega}\Delta t_{EB} - \frac{\Delta\tilde{\omega}}{2}(\Delta t_{EA} + \Delta t_{BA}) \\ & \mp \tilde{\omega}\cdot(\delta\tau_i(t) - \delta\dot{\tau}_i(t)\cdot\Delta t_{EA} - \delta\tau_j(t) + \delta\dot{\tau}_j(t)\cdot\Delta t_{BA}) \\ & - \frac{\Delta\tilde{\omega}}{2}(\delta\tau_i(t) - \delta\dot{\tau}_i(t)\cdot\Delta t_{EA} - \delta\tau_j(t) + \delta\dot{\tau}_j(t)\cdot\Delta t_{BA}) \\ & + \mathrm{const.}, \end{aligned} \tag{50}$$

where Δt_{EB} represents the difference between the photon travel time from the transmitting satellite to the photodiode on the receiving satellite and the travel time from the local laser to the photodiode on the receiver. It can be separated into the expected value of the instantaneous distance ρ_{inst} and the relativistic time delay of the photon between the satellites, represented by $\Delta t_{PQ,\mathrm{corr}}$. In an ideal situation, the ideal value and the actual measured value are assumed to be equal $\Delta t_{EB} = \Delta t_{EA} - \Delta t_{BA} = \rho_{\mathrm{inst}}(t)/c_0 + \Delta t_{PQ,\mathrm{corr}} = \Delta t_{PQ}$, where c_0 represents the speed of light in a vacuum. The variable Δt_{PQ} denotes the time taken for light to propagate between hypothetical events P and Q. Specifically, it represents the coordinate time between these two events when a photon is emitted from the centroid of the transmitting satellite and received at the centroid of the receiving satellite in the GCRS system. Considering these terms in Eq. (50), the one-way ranging (OWR) phase expression can be obtained as

$$\begin{aligned} \varphi^{(\mathrm{OWR})}_{\mathrm{PM}|j}(t) = {} & \mp\tilde{\omega}\cdot\left[\frac{\rho_{\mathrm{inst}}(t)}{c_0} + (1 - \delta\dot{\tau}_i(t))\cdot\Delta t_{PQ,\mathrm{corr}} + \delta\tau_i(t)\right. \\ & -\delta\dot{\tau}_i(t)\cdot\left(\frac{\rho_{\mathrm{inst}}(t)}{c_0} + \Delta t_{BA}\right) \\ & \left.-\delta\tau_j(t) + \delta\dot{\tau}_j(t)\cdot\Delta t_{BA}\right] \\ & -\frac{\Delta\tilde{\omega}}{2}\cdot\left\{-2t + \left(\frac{\rho_{\mathrm{inst}}(t)}{c_0} + 2\Delta t_{BA}\right)\right. \\ & + (1 - \delta\dot{\tau}_i(t))\cdot\Delta t_{PQ,\mathrm{corr}} \\ & + \delta\tau_i(t) - \delta\dot{\tau}_i(t)\cdot\left(\frac{\rho_{\mathrm{inst}}(t)}{c_0} + \Delta t_{BA}\right) \\ & \left.+\delta\tau_j(t) - \delta\dot{\tau}_j(t)\cdot\Delta t_{BA}\right\} + \mathrm{const.} \end{aligned} \tag{51}$$

4.2. Dual one-way ranging

As shown in Fig. 2, the dual one-way ranging (DOWR) can be considered as a superposition of two one-way rangings, one-way ranging from S/C i to S/C j and one-way ranging from S/C j to S/C i. In the S/C j to S/C i one-way ranging, the phase of the S/C i phasemeter can be obtained in an analogous OWR analysis by following rules:

(a) For the situation where the functions of two satellites i and j are exchanged, it is reflected in the formula as exchanging all subscripts i and j.

(b) Since the frequency order is unchanged during the exchange, the signs $\pm$ and $\mp$ need to be exchanged in the expression.

(c) All event labels like $A, B, \ldots$ are replaced by the corresponding primed variables. According to the above notation, we can obtain the expression of the phase of the S/C i phasemeter corresponding to Eq. (51)

$$\begin{aligned} \varphi^{(\mathrm{OWR})}_{\mathrm{PM}|i}(t) = {} & \pm\tilde{\omega}\cdot\left[\frac{\rho_{\mathrm{inst}}(t)}{c_0} + (1 - \delta\dot{\tau}_j(t))\cdot\Delta t_{P'Q',\mathrm{corr}}\right. \\ & +\delta\tau_j(t) - \delta\dot{\tau}_j(t)\cdot\left(\frac{\rho_{\mathrm{inst}}(t)}{c_0} + \Delta t_{B'A'}\right) \\ & \left.-\delta\tau_i(t) + \delta\dot{\tau}_i\cdot\Delta t_{B'A'}\right] \end{aligned}$$

$$
\begin{aligned}
&-\frac{\Delta\tilde{\omega}}{2}\cdot\left\{-2t+\left(\frac{\rho_{\text{inst}}(t)}{c_0}+2\Delta t_{B'A'}\right)\right.\\
&+(1-\delta\dot{\tau}_j(t))\cdot\Delta t_{P'Q',\text{corr}}\\
&+\delta\tau_j(t)-\delta\dot{\tau}_j(t)\cdot\left(\frac{\rho_{\text{inst}}(t)}{c_0}+\Delta t_{B'A'}\right)\\
&\left.+\delta\tau_i(t)-\delta\dot{\tau}_i\cdot\Delta t_{B'A'}\right\}+\text{const.},
\end{aligned}
\tag{52}
$$

where the above formula defaults to $\bar{\omega}_{i|i}>\bar{\omega}_{j|j}$. It is assumed that the relative velocity $\dot{\rho}_{\text{inst}}$ between the two S/C is low enough that the Doppler frequency shift does not change the frequency order $(\dot{\rho}_{\text{inst}}/c_0)\cdot\bar{\omega}_{i|i}<\left|\bar{\omega}_{j|j}-\bar{\omega}_{i|i}\right|$. Combining Eqs. (51) and (52), the phase expression of DOWR becomes

$$
\begin{aligned}
\Theta(t) &= \varphi^{(\text{OWR})}_{\text{PM}|i}(t)-\varphi^{(\text{OWR})}_{\text{PM}|j}(t)\\
&=\pm\tilde{\omega}\cdot\left\{\frac{2\rho_{\text{inst}}(t)}{c_0}+\left[(1-\delta\dot{\tau}_j(t))\cdot\Delta t_{P'Q',\text{corr}}\right.\right.\\
&\quad\left.+(1-\delta\dot{\tau}_i(t))\cdot\Delta t_{PQ,\text{corr}}\right]\\
&\quad-\delta\dot{\tau}_j(t)\cdot\left(\frac{\rho_{\text{inst}}(t)}{c_0}+\Delta t_{B'A'}-\Delta t_{BA}\right)\\
&\quad\left.-\delta\dot{\tau}_i(t)\cdot\left(\frac{\rho_{\text{inst}}(t)}{c_0}+\Delta t_{BA}-\Delta t_{B'A'}\right)\right\}\\
&\quad-\frac{\Delta\tilde{\omega}}{2}\cdot\left\{2(\Delta t_{B'A'}-\Delta t_{BA})+\left[(1-\delta\dot{\tau}_j(t))\cdot\Delta t_{P'Q',\text{corr}}\right.\right.\\
&\quad\left.-(1-\delta\dot{\tau}_i(t))\cdot\Delta t_{PQ,\text{corr}}\right]\\
&\quad-\delta\dot{\tau}_j(t)\cdot\left(\frac{\rho_{\text{inst}}(t)}{c_0}+\Delta t_{B'A'}-\Delta t_{BA}\right)\\
&\quad\left.+\delta\dot{\tau}_i(t)\cdot\left(\frac{\rho_{\text{inst}}(t)}{c_0}+\Delta t_{BA}-\Delta t_{B'A'}\right)\right\}\\
&\quad+\text{const.}
\end{aligned}
\tag{53}
$$

The DOWR phase expression can be converted into an equivalent distance by the following formula:

$$
\rho_\Theta(t)=\frac{c_0\cdot\Theta(t)}{\mp2\cdot\tilde{\omega}_{\text{est}}},
\tag{54}
$$

where $\tilde{\omega}_{\text{est}}$ represents the best estimate of the average angular frequency of both satellites. The average laser angular frequency of different satellites is denoted by $\bar{\omega}_{i|i}$ and $\bar{\omega}_{j|j}$, which are functions of coordinate time. The timing problem becomes complicated due to the theory of relativity in the context of curved space–time. The first step to obtain the instantaneous distance is $\rho_\Theta(t)$, which separates the time delay part from the expression

$$
\begin{aligned}
\Delta\rho_{\text{DOWR,corr}}(t) &= \frac{c_0}{\mp2\cdot\tilde{\omega}_{\text{est}}}\left\{\pm\tilde{\omega}\cdot\left[(1-\delta\dot{\tau}_j)\cdot\Delta t_{P'Q',\text{corr}}\right.\right.\\
&\quad\left.+(1-\delta\dot{\tau}_i)\cdot\Delta t_{PQ,\text{corr}}\right]\\
&\quad-\frac{\Delta\tilde{\omega}}{2}\cdot\left[\Delta t_{P'Q',\text{corr}}-\Delta t_{PQ,\text{corr}}\right.\\
&\quad\left.\left.-\delta\dot{\tau}_j\cdot\Delta t_{P'Q',\text{corr}}+\delta\dot{\tau}_i\cdot\Delta t_{PQ,\text{corr}}\right]\right\}.
\end{aligned}
\tag{55}
$$

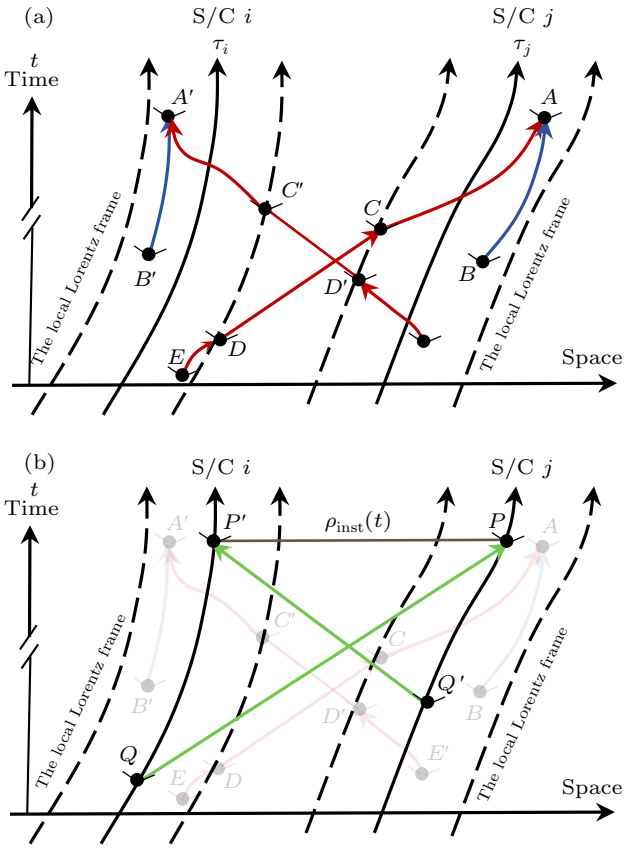


Fig. 2. (a) The space–time diagram of the actual optical path and (b) the space–time diagram of the ideal optical path.

4.3. Transponder-based ranging

Figure 3 shows the space–time diagram of the optical path of transponder-based ranging. Each satellite performs light emission and reception, with both conducting interferometric phase readout, similar to DOWR. Equation (50) can be used to obtain the interferometric phase of the slave satellite at time t_A

$$
\begin{aligned}
\varphi^{(\text{OL})}_{\text{PM}|S}(t_A) &= \pm\bar{\omega}_{M|M}\cdot\tau_M(t_A-\Delta t_{EA})\\
&\quad\mp\bar{\omega}_{S|S}\cdot\tau_S(t_A-\Delta t_{BA})+\text{const.}
\end{aligned}
\tag{56}
$$

The $\varphi^{(\text{OWR})}_{\text{PM}|j}(t)$ is further rewritten by using Eq. (51) (namely, $t\to t_A|i\to M|j\to S$)

$$
\begin{aligned}
&\varphi^{(\text{OL})}_{\text{PM}|S}(t_A)\\
&=\mp\tilde{\omega}\cdot\left\{\frac{\rho_{\text{inst}}(t_A)}{c_0}+(1-\delta\dot{\tau}_M(t_A))\cdot\Delta t_{PQ,\text{corr}}\right.\\
&\quad\left.+\delta\tau_M(t_A)-\delta\dot{\tau}_M(t_A)\cdot\left(\frac{\rho_{\text{inst}}(t_A)}{c_0}+\delta t_{EB,\text{ifo}}+\Delta t_{BA}\right)\right.
\end{aligned}
$$

$$
\begin{aligned}
&-\delta\tau_S(t_A)+\delta\dot{\tau}_S(t_A)\cdot\Delta t_{BA}\Big\}\\
&-\frac{\Delta\tilde{\omega}}{2}\cdot\Big\{-2t_A+\left(\frac{\rho_{\rm inst}(t_A)}{c_0}+2\Delta t_{BA}\right)\\
&+(1-\delta\dot{\tau}_M(t_A))\cdot\Delta t_{PQ,\rm corr}\\
&+\delta\tau_M(t_A)-\delta\dot{\tau}_M(t_A)\cdot\left(\frac{\rho_{\rm inst}(t_A)}{c_0}+\Delta t_{BA}\right)\\
&+\delta\tau_S(t_A)-\delta\dot{\tau}_S(t_A)\cdot\Delta t_{BA}\Big\}+\text{const.}
\end{aligned}
\tag{57}
$$

Likewise, the laser frequency of the master satellite is greater than that of the slave satellite, and the Doppler frequency shift effect does not alter the order of the laser frequency. The slave satellite's S/C uses a feedback control loop, specifically a phase-locked loop,

$$
\varphi^{(\rm CL)}_{\rm PM|S}\left(\tau_S\left(t_A\right)\right)=\omega_{{\rm off},S}\cdot\tau_S\left(t_A\right)+\text{const.}
\tag{58}
$$

The phase of the slave satellite closely follows a linear function with a slope of $\omega_{{\rm off},S}$, and the zero point of this function is obtained by imprinting the phase information of the laser emitted by the master satellite onto the phase information of the slave satellite, which is then reflected back to the master satellite. By using the world line of light as a constant phase line and considering the Lorentz invariance of phase, it is possible to obtain

$$
\begin{aligned}
\Phi_B\left(\tau_S\left(t_B\right)\right) &= +\Phi_{\rm RX}\left(\tau_S\left(t_A\right)\right)\mp\omega_{{\rm off},S}\cdot\tau_S\left(t_A\right)\\
&= +\bar{\omega}_{M|M}\cdot\tau_M\left(t_E\right)\mp\omega_{{\rm off},S}\cdot\tau_S\left(t_A\right).
\end{aligned}
\tag{59}
$$

The reflection phase at event A is denoted by $\Phi_{\rm RX}\left(\tau_S\left(t_A\right)\right)$. As with DOWR, it is necessary that the Doppler frequency shift is smaller than the offset frequency, so that the relative motion between the satellites cannot reverse the frequency order, specifically $\left(\dot{\rho}_{\rm inst}/c_0\right)\bar{\omega}_{M|M}<\omega_{{\rm off},S}$. The laser signal reflected from the slave satellite is transmitted back to the master satellite, where this signal interferes with the local laser to obtain the beat frequency phase

$$
\begin{aligned}
\varphi_{\rm PM|M}\left(t_{A'}\right) &= \pm\bar{\omega}_{M|M}\cdot\tau_M\left(t_{A'}-\Delta t_{B'A'}\right)\\
&\quad\mp\bar{\omega}_{M|M}\cdot\tau_M\left(t_{A'}-\Delta t_{EA'}\right)\\
&\quad+\omega_{{\rm off},S}\cdot\tau_S\left(t_{A'}-\Delta t_{AA'}\right)+\text{const.}
\end{aligned}
\tag{60}
$$

The $\Delta t_{EB'}$ can be written as a combination of the related term and the corrected term of the instantaneous ranging term $\rho_{\rm inst}$

$$
\Delta t_{EB'}=\frac{2\rho_{\rm inst}}{c_0}+\Delta t_{QPR,\rm corr}=\Delta t_{QPR}=\Delta t_{EA'}-\Delta t_{B'A'},
\tag{61}
$$

where $\Delta t_{QPR,\rm corr}$ represents the relativistic delay correction for the round-trip process between satellites, and Δt_{QPR} represents the gravitational delay correction for the photon from point Q to point P and then to point R along the actual trajectory of the optical path. By using Eq. (61), Eq. (60) can be rewritten as an expression with information of instantaneous ranging

$$
\begin{aligned}
&\bar{\omega}_{M|M}\cdot\tau_M\left(t_{A'}-\Delta t_{B'A'}\right)-\bar{\omega}_{M|M}\cdot\tau_M\left(t_{A'}-\Delta t_{EA'}\right)\\
&=\bar{\omega}_{M|M}\cdot\left(1-\delta\dot{\tau}_M\left(t_{A'}\right)\right)\cdot\left(\frac{2\rho_{\rm inst}}{c_0}+\Delta t_{QPR,\rm corr}\right).
\end{aligned}
\tag{62}
$$

Considering the time difference $\Delta t_{AA'}$, it can be expressed as

$$
\begin{aligned}
\Delta t_{AA'} &= \Delta t_{E'B'}+\Delta t_{B'A'}-\Delta t_{E'A}\\
&= \frac{\rho_{\rm inst}\left(t_{A'}\right)}{c_0}+\Delta t_{PQ,\rm corr}\left(t_{A'}\right)+\Delta t_{B'A'}-\Delta t_{E'A}.
\end{aligned}
\tag{63}
$$

Based on the above analysis, Eq. (57) can be rewritten as

$$
\begin{aligned}
&\varphi_{\rm PM|M}\left(t\right)\\
&=\pm\bar{\omega}_{M|M}\cdot\left(\frac{2\rho_{\rm inst}}{c_0}+\left(1-\delta\dot{\tau}_M\left(t\right)\right)\cdot\Delta t_{QPR,\rm corr}\right.\\
&\quad\left.-\delta\dot{\tau}_M\left(t\right)\cdot\frac{2\rho_{\rm inst}}{c_0}\right)-\omega_{{\rm off},S}\cdot\Big\{-t+\frac{\rho_{\rm inst}\left(t\right)}{c_0}\\
&\quad+\left(1-\delta\dot{\tau}_S\left(t\right)\right)\cdot\Delta t_{PQ,\rm corr}\left(t\right)+\Delta t_{B'A'}-\Delta t_{E'A}+\delta\tau_S\left(t\right)\\
&\quad\left.-\delta\dot{\tau}_S\left(t\right)\cdot\left(\frac{\rho_{\rm inst}\left(t\right)}{c_0}+\Delta t_{B'A'}-\Delta t_{E'A}\right)\right\}+\text{const.}
\end{aligned}
\tag{64}
$$

The phase observations in transponder-based ranging schemes can be converted to equivalent inter-satellite distances

$$
\rho_{MS}=\frac{c_0\cdot\varphi_{\rm PM|M}\left(t\right)-c_0\cdot\varphi^{(\rm CL)}_{\rm PM|S}\left(t\right)}{\pm2\tilde{\omega}_{\rm est}}+\text{const.},
\tag{65}
$$

where $\tilde{\omega}_{\rm est}$ is the best estimate of the mean angular frequency of the two satellites, namely, $\tilde{\omega}=\left(\bar{\omega}_{M|M}+\bar{\omega}_{S|S}\right)/2$. This method is to pull the phase after the phase-locked loops of the slave satellite to the same coordinate time as the master satellite in the GCRS coordinate system, and then calculate the difference. Another approach is based on delaying the phase of the slave satellites

$$
\begin{aligned}
\rho_{MS} &= \frac{c_0\cdot\varphi_{\rm PM|M}\left(t\right)-c_0\cdot\varphi^{(\rm CL)}_{\rm PM|S}\left(t-\frac{\rho_{\rm inst,est}(t)}{c_0}\right)}{\pm2\tilde{\omega}_{M|M,\rm est}}\\
&\quad+\text{const.},
\end{aligned}
\tag{66}
$$

where $\rho_{\rm inst,est}(t)$ is the estimated value of $\rho_{\rm inst}(t)$. The denominator of this expression is the estimated frequency $\tilde{\omega}_{M|M,\rm est}$ of the master satellite's laser, and this method can eliminate the error caused by the inaccurate estimation of the slave satellite's laser frequency. As the same analysis of Eq. (55), the time delay part can be expressed as

$$
\begin{aligned}
\Delta\rho_{\rm TBR,corr} &= \frac{c_0}{\pm2\tilde{\omega}_{M|M,\rm est}}\big[\pm\bar{\omega}_{M|M}\cdot\left(1-\delta\dot{\tau}_M\left(t\right)\right)\cdot\Delta t_{QPR,\rm corr}\\
&\quad-\omega_{{\rm off},S}\cdot\left(1-\delta\dot{\tau}_S\left(t\right)\right)\cdot\Delta t_{PQ,\rm corr}\big].
\end{aligned}
\tag{67}
$$

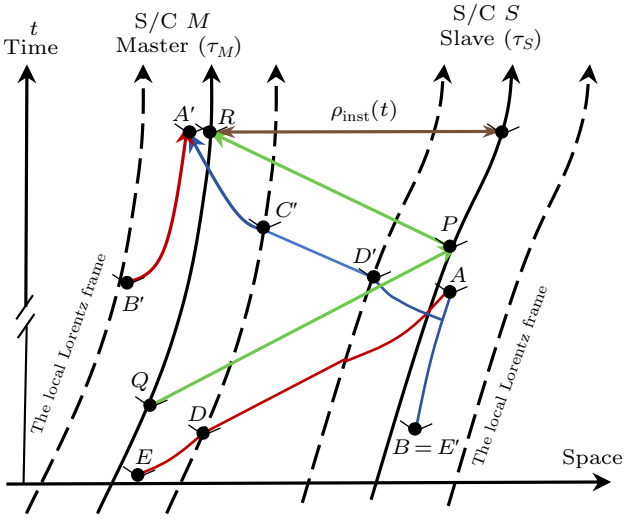


Fig. 3. Space–time diagram of master and slave satellites.

5. Estimation of gravitational delay in GRACE-FO-like missions

The gravitational delay leads to an extra delay in the light propagation, which may affect the results of laser ranging in the high-recision space missions. In this section, we estimate the influences of gravitational delays on the laser ranging of the GRACE-FO-like missions. Considering the ranging accuracy in the future space missions, the gravitational delays are evaluated to the level of picometer. The orbit parameters are those of the GRACE-FO mission, as shown in Table 1. By using some useful relations for the Keplerian orbits (Eqs. (A1)–(A4) in Appendix A), the expressions for the world function can be expanded in terms of orbital parameters to the order e^2

$$\mathcal{T}_e^{(\rm Shapiro)} = \frac{GM(1+\gamma)\,d_{AB}}{ac^3} \times \left(1+e\cos\omega_G t+e^2\cos^2\omega_G t\right), \tag{68}$$

$$\mathcal{T}_e^{(J_2)} = \frac{GM(1+\gamma)J_2R_{\rm E}^2}{2c^3}\frac{d_{AB}}{a^3}(2\cos^2\theta-\sin^2\theta) \times \left(1+3e\cos\omega_G t+3e^2\cos^2\omega_G t\right), \tag{69}$$

$$\mathcal{T}_e^{(J_3)} = \frac{GM(1+\gamma)J_3R_{\rm E}^3 d_{AB}\cos\theta}{2a^4c^3}\left[1+4e\cos\omega_G t +4e^2\cos^2\omega_G t+(\sin^2\theta)5e^2\cos^2\omega_G t\right], \tag{70}$$

$$\mathcal{T}_e^{(J_4)} = (-1)\frac{GM(1+\gamma)}{c^3}J_4R_{\rm E}^4\left\{\frac{-d_{AB}}{a^5}\cos^4\theta \times(1+5e\cos\omega_G t+5e^2\cos^2\omega_G t) +\frac{d_{AB}}{4a^5}\cos^2\theta\sin^2\theta\left(7+35e\cos\omega_G t+59e^2\cos^2\omega_G t\right) -\frac{d_{AB}}{4a^5}\sin^4\theta\left(1+5e\cos\omega_G t+12e^2\cos^2\omega_G t\right) +\frac{d_{AB}}{8a^5}\sin^2\theta(5\cos^2\theta-1) \times(1+5e\cos\omega_G+5e^2\cos^2\omega_G t)\right\}, \tag{71}$$

$$\mathcal{T}_e^{(S)} = \frac{GS(\gamma+1)\sin\theta}{ac^4}\frac{d_{AB}}{a} \times\left(\frac{3}{2}+2e\cos\omega_G t+\frac{e^2}{2}\cos^2\omega_G t\right), \tag{72}$$

$$\mathcal{T}_e^{(K_1)} = \frac{GM(\gamma+1)K_1R_{\rm E}S}{c^4}\frac{d_{AB}}{a^3}\cos\theta \times\left(1+3e\cos\omega_G t+e^2\cos^2\omega_G t\right), \tag{73}$$

$$\mathcal{T}_e^{(G^2)} = -\frac{G^2M^2R_{AB}}{4c^5a^2}[4\beta-8-8\gamma-3\delta] \times\left(1+2e\cos\omega_G t+e^2\cos^2\omega_G t\right)\frac{\arccos(\boldsymbol{n}_A\cdot\boldsymbol{n}_B)}{\sqrt{1-(\boldsymbol{n}_A\cdot\boldsymbol{n}_B)^2}} -\frac{G^2M^2R_{AB}}{c^5}\left[\frac{(1+\gamma)^2}{a^2}\left(1+3e\cos\omega_G t \times+3e^2\cos^2\omega_G t+\frac{e^2}{2}\sin^2\omega_G t\right)\right], \tag{74}$$

where d_{AB} is the interspacecraft range, e is the orbital eccentricity, θ is the angle from the axis of the Earth rotation to orbital plane, $\omega_G=(1/2)(\omega_A+\omega_B)$, $\omega_{A/B}$ is the orbital angular frequency of satellite A/B, and a is the semi-major axis of the orbit.

Table 1. The parameters of the GRACE-FO mission.

Parameter	Value
Earth's mass	$M=5.9722\times10^{24}$ kg
Gravitational constant	$G=6.67\times10^{-11}$ m/(kg·s^2)
The eccentricity of Earth	0.0033528
Interspacecraft range	$d_{AB}=270$ km
Earth radius	$R_{\rm E}=6371$ km

Based on those orbit parameters in Table 1, one can estimate the gravitational delay effects. For the estimation of the gravitational delay, the maximum term is the Shapiro term, which corresponds to the relativistic post-Newton parameter $\gamma=\beta=\epsilon=1$

$$c\mathcal{T}_e^{(\rm Shapiro)}\sim 351\times\left(1+10^{-3}\cos\omega_G t+10^{-6}\cos^2\omega_G t\right)\ \mu\text{m}, \tag{75}$$

and after some calculations, the other terms are given by

$$c\mathcal{T}_e^{(J_2)}\sim(410\cos^2\theta-205\sin^2\theta)(1+3\times10^{-3}\cos\omega_G t)\ \text{nm}, \tag{76}$$

$$c\mathcal{T}_e^{(J_3)}\sim-383\cos\theta\ \text{pm}, \tag{77}$$

$$c\mathcal{T}_e^{(J_4)} \sim -430\left[\cos^4\theta - \frac{7}{4}\cos^2\theta\sin^2\theta + \frac{1}{4}\sin^4\theta - \frac{1}{8}\sin^2\theta(5\cos^2\theta - 1)\right] \text{pm}, \quad (78)$$

$$c\mathcal{T}_e^{(S)} \sim 252\sin\theta \text{ pm}, \quad (79)$$

$$c\mathcal{T}_e^{(K_1)} \sim \frac{GM(\gamma+1)K_1R_{\rm E}S}{c^4}\frac{d_{AB}}{a^3} \sim 10^{-1} \text{ pm}. \quad (80)$$

The above contributions may need to be considered for picometer level ranging. The contribution of higher-order mass multipole moment is given by $c\Gamma_e^{(J_4)} \sim 10^{-3}$pm, which is negligible. To calculate the contribution of the G^2 term, one can use the vector relation with L'Hopital's rule

$$\lim_{\boldsymbol{n}_A\cdot\boldsymbol{n}_B\to 1}\frac{\arccos(\boldsymbol{n}_A\cdot\boldsymbol{n}_B)}{\sqrt{1-(\boldsymbol{n}_A\cdot\boldsymbol{n}_B)^2}} = \lim_{\boldsymbol{n}_A\cdot\boldsymbol{n}_B\to 1}\left(\frac{1}{\boldsymbol{n}_A\cdot\boldsymbol{n}_B}\right) = 1. \quad (81)$$

Therefore, the G^2 term becomes $c\Gamma_e^{(G^2)} \sim 10^{-1}$ pm, which is nonnegligible.

In laser ranging space missions, a laser with a wavelength of $\lambda = 1064$ nm is typically selected. The corresponding laser frequency can be obtained as $\tilde{\omega} = c/\lambda = 282$ THz. Furthermore, the beat frequency is usually set to $\Delta\tilde{\omega} = 10$ MHz, giving us $\Delta\tilde{\omega}/\tilde{\omega} = 3.54\times10^{-8}$. Considering the desired magnitude of 1 pm, we must take into account the coupling effect of the beat frequency term and the first-order correction of the time delay Shapiro term

$$c\Gamma_e^{(\rm Shapiro)}\frac{\Delta\tilde{\omega}}{\tilde{\omega}} \sim 12.4\left(1+10^{-3}\cos\omega_G t\right) \text{ pm}. \quad (82)$$

This effect is of significant importance for the magnitude of phase modulation, as the beat frequency term is exclusively reserved for the Shapiro term and cannot be overlooked.

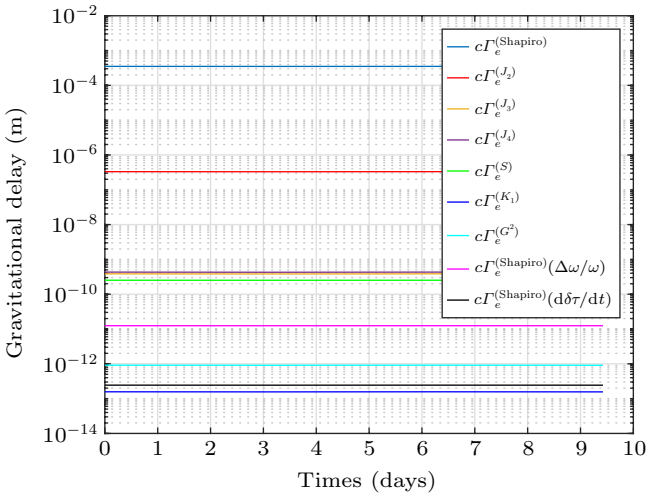


Fig. 4. Various terms of the gravitational delay.

Table 2. The estimations of the gravitational delay on the GRACE-FO-like missions.

Terms	Parameter	Magnitude
Shapiro	$c\mathcal{T}_e^{(\rm Shapiro)}$	351 μm
Earth mass multipolar moment J_2	$c\mathcal{T}_e^{(J_2)}$	$(410\cos^2\theta - 205\sin^2\theta)$ nm
Earth mass multipolar moment J_3	$c\mathcal{T}_e^{(J_3)}$	$-383\cos\theta$ pm
Earth mass multipolar moment J_4	$c\mathcal{T}_e^{(J_4)}$	$-430[\cos^4\theta - \frac{7}{4}\cos^2\theta\sin^2\theta + \frac{1}{4}\sin^4\theta - \frac{1}{8}\sin^2\theta(5\cos^2\theta-1)]$ pm
Earth's rotation S	$c\mathcal{T}_e^{(S)}$	$252\sin\theta$ pm
Earth's rotation expansion K_1	$c\mathcal{T}_e^{(K_1)}$	10^{-1} pm
Gravitational 2PN term	$c\mathcal{T}_e^{(G^2)}$	10^{-1} pm
Coupled effect of Shapiro and beat frequency	$c\mathcal{T}_e^{(\rm Shapiro)}\frac{\Delta\tilde{\omega}}{\tilde{\omega}}$	12.4 pm
Coupled effect of Shapiro and Doppler effect	$c\mathcal{T}_e^{(\rm Shapiro)}\delta\dot{\tau}(t)$	10^{-1} pm

Regarding the effect caused by the conversion between proper time and coordinate time, it can be expressed as

$$\delta\dot{\tau}(t) = \frac{v^2}{2c^2} + \frac{W}{c^2} + \frac{\gamma W v^2}{c^4} - \frac{2(\gamma+1)}{c^4}(\boldsymbol{W}\cdot\boldsymbol{v}) - \frac{\beta W^2}{c^4}, \quad (83)$$

where the first term is the time dilation effect and the second term is the gravitational redshift. It can be inferred that these two terms are coupled to the Shapiro term, resulting in a subpicometer effect

$$c\Gamma_e^{(\rm Shapiro)}\delta\dot{\tau}(t) \sim \frac{GM(1+\gamma)d_{AB}}{ac^2}\left(\frac{v^2}{2c^2} + \frac{GM}{R_{\rm E}c^2}\right) \sim 10^{-1} \text{ pm}. \quad (84)$$

For a summary, figure 4 presents an intuitive schematic diagram for various terms of the gravitational delay. In Fig. 4, the light blue line represents the contribution of Earth's mass $c\Gamma_e^{(\rm Shapiro)}$. The red, brown and purple lines indicate the contributions of Earth's mass multipole moments J_2, J_3, and J_4, respectively. The green and dark blue lines depict the contributions of Earth's rotation. The pink line is the contribution of the coupled effect of the Shapiro term and the beat frequency. The black line represents the coupled effect of the Shapiro term with the Doppler effect. And the sky blue line represents the contribution of gravitational 2PN terms. The estimated gravitational delays are listed in Table 2.

In the case of dual one-way ranging and transponder-based ranging, the formula can be simplified as follows: $\Delta t_{QPR,\rm corr}/2 = \Delta t_{P'Q',\rm corr} = \Delta t_{PQ,\rm corr} = \Delta t_{\rm corr}$ and $\tilde{\omega}_{\rm est} = \tilde{\omega}$ are not taken into account in this study to estimate only the order

of magnitude of the measurements. Thus, we have

$$\Delta\rho_{\mathrm{DOWR,corr}} = -c_0\mathcal{T}_e + c_0\mathcal{T}_e^{(\mathrm{Shapiro})}\left(\frac{v^2}{2c^2}+\frac{GM_{\mathrm{E}}}{R_{\mathrm{E}}c^2}\right), \quad (85)$$

$$\Delta\rho_{\mathrm{TBR,corr}} = c_0\mathcal{T}_e \mp \frac{\Delta\tilde{\omega}}{\tilde{\omega}}\frac{c_0\mathcal{T}_0^{(\mathrm{Shapiro})}}{2} - c_0\mathcal{T}_e^{(\mathrm{Shapiro})}\left(\frac{v^2}{2c^2}+\frac{GM_{\mathrm{E}}}{R_{\mathrm{E}}c^2}\right). \quad (86)$$

Comparing one-way ranging (OWR) and transponder-based ranging (TBR) shows that OWR experiences fewer coupling terms of the Shapiro effect in both beat frequency and time delay than TBR.

6. Conclusion

With the rapid advancement of laser ranging technology, various near-Earth space missions may use high-precision interferometers for scientific experiments and a precise relativistic model for observables is required. Therefore, it is important to evaluate the influences of the gravitational delays on the GRACE-FO-like missions. Within the post-Newton approximation, we utilize the Synge world function method to study the light propagation in the gravitational field. In the GCRS, the time transfer delay is expanded to the order of c^{-5} for the light propagation in Earth's gravitational field, which corresponds to the gravitational delay effects to the order of c^{-4}. Further considering the possible ranging requirements of GRACE-FO-like missions, we investigate the influences of gravitational delays on three ranging techniques, including one-way ranging, dual one-way ranging, and transponder-based ranging.

Based on the Keplerian orbits, the semi-analytic expressions of gravitational delay are derived in the terms of the orbital parameters. This formulation allows us to analyze the gravitational effects on the GRACE-FO-like missions. Based on the concept and parameters of GRACE-FO-like, we evaluate the influences of the gravitational delays on the laser ranging. For the accuracy of picometer level, it includes the contributions of the Earth's mass, mass multipole moments, Earth's rotation, and gravitational 2PN term. Furthermore, we investigate the coupling effects of the Shapiro effect to beat frequency, and the Shapiro effect to Doppler shift, whose contributions may be nonnegligible in the picometer accuracy. Finally, we estimate the magnitudes of various terms on the range, including contributions of the Earth's mass, mass multipole moments, Earth's rotation, gravitational 2PN term, and coupling effects of Shapiro to beat frequency and Doppler shift. Our result is also applicable to relativistic analysis of analogous space missions.

Appendix A: Some useful relations for Keplerian orbits

In this appendix, we introduce some useful relations to evaluate the magnitudes of various gravitational delays that involve combinations of orbital parameters of GRACE-FO-like satellites. We assume that two satellites are in the same Keplerian orbit around the Earth, with the semi-major axis $a = R_{\mathrm{E}} + h_G$ (where h_G is the orbital altitude) and eccentricity e ($e \ll 1$), but with different eccentric anomalies $\mathcal{E}_A$ and $\mathcal{E}_B$. However, since the model used does not take into account the influence of non-gravitational and relativistic effects on the orbit, this assessment has practical significance only in terms of order of magnitude, and precise values cannot be calculated. Based on these assumptions, the expression for the associated quantity of satellite A is as follows:

$$\boldsymbol{r}_A = a\left(\cos\mathcal{E}_A - e, \sqrt{1-e^2}\sin\mathcal{E}_A\right), \quad (A1)$$

$$r_A = a(1-e\cos\mathcal{E}_A), \quad (A2)$$

$$\boldsymbol{n}_A = \left(\frac{\cos\mathcal{E}_A - e}{1-e\cos\mathcal{E}_A}, \frac{\sqrt{1-e^2}\sin\mathcal{E}_A}{1-e\cos\mathcal{E}_A}\right), \quad (A3)$$

$$\boldsymbol{v}_A = \frac{\sqrt{GMa}}{r_A}\left(-\sin\mathcal{E}_A, \sqrt{1-e^2}\cos\mathcal{E}_A\right). \quad (A4)$$

For simplicity, we introduce two angles α_{AB} and β_{AB}

$$\begin{cases} \mathcal{E}_A = \beta_{AB} - \alpha_{AB}, \\ \mathcal{E}_B = \alpha_{AB} + \beta_{AB}, \end{cases} \quad (A5)$$

where

$$\alpha_{AB} = \frac{d_{AB}}{2a} + O\left(d_{AB}^3, e^2\right), \quad \beta_{AB} = \omega_G t + O\left(d_{AB}, e\right), \quad (A6)$$

$$\omega_G = \frac{1}{2}(\omega_A + \omega_B) + O(e) \equiv \sqrt{\frac{GM}{a^3}} + O(e). \quad (A7)$$

Then some relations between two spacecrafts can be determined using Eqs. (A1)–(A4)

$$R_{AB} = 2a\sin\alpha_{AB}\sqrt{1-e^2\cos^2\beta_{AB}}, \quad (A8)$$

$$\boldsymbol{R}_{AB} = 2a\sin\alpha_{AB}\left(-\sin\beta_{AB}, \sqrt{1-e^2}\cos\beta_{AB}\right), \quad (A9)$$

$$\boldsymbol{n}_{AB} = \frac{1}{\sqrt{1-e^2\cos^2\beta_{AB}}}\left(-\sin\beta_{AB}, \sqrt{1-e^2}\cos\beta_{Ab}\right). \quad (A10)$$

The z-axis represents the plane of rotation of the satellite around the Earth, and θ represents the angle between the plane of rotation around the Earth and the axis of rotation of the Earth, $\boldsymbol{k}\cdot\boldsymbol{n}_A = \boldsymbol{k}\cdot\boldsymbol{n}_B = \cos\theta$. Since the eccentricity e is small enough, the above quantity can be expanded by a small quantity $e\cos\omega_G t$. To analyze possible contributions to the picometer level, some terms in the gravitational delays are carried out to the second order terms, resulting in

$$v_A^2 = \frac{GM}{a}\left(1 + 2e\cos\mathcal{E}_A - 2e^2\cos^2\mathcal{E}_A\right), \quad (A11)$$

$$\ln\left(\frac{r_A+r_B+R_{AB}}{r_A+r_B-R_{AB}}\right)$$

$$= \frac{d_{AB}}{a}\times\left(1+e\cos\omega_G t+e^2\cos^2\omega_G t\right), \tag{A12}$$

$$\frac{1}{r_A+r_B+R_{AB}}-\frac{1}{r_A+r_B-R_{AB}}$$

$$= \frac{-2R_{AB}}{(r_A+r_B)^2-R_{AB}^2}$$

$$= \frac{-d_{AB}}{2a^2}\left(1+2e\cos\omega_G t+2e^2\cos^2\omega_G t\right), \tag{A13}$$

$$\frac{1}{(r_A+r_B+R_{AB})^2}-\frac{1}{(r_A+r_B-R_{AB})^2}$$

$$= \frac{-d_{AB}}{2a^3}\left(1+3e\cos\omega_G t+3e^2\cos^2\omega_G t\right), \tag{A14}$$

$$\frac{1}{(r_A+r_B+R_{AB})^3}-\frac{1}{(r_A+r_B-R_{AB})^3}$$

$$= \frac{-3d_{AB}}{16a^4}\left(1+4e\cos\omega_G t+4e^2\cos^2\omega_G t\right), \tag{A15}$$

$$\frac{1}{r_A}+\frac{1}{r_B} = \frac{1}{a(1-e\cos\mathcal{E}_A)}+\frac{1}{a(1-e\cos\mathcal{E}_B)}$$

$$= \frac{2}{a}\left(1+e\cos\omega_G t\right), \tag{A16}$$

$$\boldsymbol{n}_A\cdot\boldsymbol{n}_B = 1-2e\cos\omega_G t-e^2\sin^2\omega_G t, \tag{A17}$$

$$\boldsymbol{n}_{AB}\times(\boldsymbol{n}_A+\boldsymbol{n}_B)$$

$$= \left(2+e^2+4e\cos\omega_G t+4e^2\cos^2\omega_G t\right)\boldsymbol{k}, \tag{A18}$$

$$\frac{d_{AB}}{R_{AB}} = \frac{1}{\sqrt{1-e^2\cos^2\beta_{AB}}} = 1+\frac{1}{2}e^2\cos^2\omega_G t. \tag{A19}$$

Acknowledgments

Project supported by the National Natural Science Foundation of China (Grant Nos. 12247150, 12305062, 12175076, and 11925503), the Post-doctoral Science Foundation of China (Grant No. 2022M721257), and the Guangdong Major Project of Basic and Applied Basic Research (Grant No. 2019B030302001).

References

[1] Abich K, Abramovici A, Amparan B, *et al.* 2019 *Phys. Rev. Lett.* **123** 031101
[2] Amaro-Seoane P, Audley H, Babak S, Baker J, *et al.* 2017 arXiv: 1702.00786
[3] Wu J, Li J and Jiang Q Q 2023 *Chin. Phys. B* **32** 090401
[4] Poncin-Lafitte C Le, Linet B and Teyssandier P 2004 *Classical and Quantum Gravity* **21** 4463
[5] Thorne K S, Misner C W and Wheeler J A 2000 *Gravitation* (Freeman San Francisco) p. 265
[6] Bertotti B, Iess L and Tortora P 2003 *Nature* **425** 374
[7] Turyshev S G, Shao M, Girerd A and Lane B 2009 *Int. J. Mod. Phys. D* **18** 1025
[8] Tso R and Bailey Q G 2010 *Phys. Rev. D* **84** 085025
[9] Kostelecký V A and Tasson J D 2011 *Phys. Rev. D* **83** 016013
[10] Qin C G, Ke J, Li Q, Chen Y F, Luo J, Tan Y J and Shao C G 2023 *Classical and Quantum Gravity* **40** 205005
[11] eLISA Consortium, *et al.* 2013 *ESA: Paris, Freance* **2013** 1
[12] Turyshev S G, Sazhin M V and Toth V T 2014 *Phys. Rev. D* **89** 105029
[13] Turyshev S G, Toth V T and Sazhin M V 2013 *Phys. Rev. D* **87** 024020
[14] Klioner S and Kopeikin S 1992 *Astron. J.* **104** 897
[15] Linet B and Teyssandier P 2013 *Classical and Quantum Gravity* **30** 175008
[16] Kopeikin S and Mashhoon B 2002 *Phys. Rev. D* **65** 064025
[17] He G and Lin W 2016 *Phys. Rev. D* **94** 063011
[18] Jiang C and Lin W 2018 *Phys. Rev. D* **97** 024045
[19] Ghosh S and Bhattacharyya A 2022 *J. Cosmol. Astropart. Phys.* **2022** 006
[20] Teyssandier P 1978 *Phys. Rev. D* **18** 1037
[21] Zschocke S 2015 *Phys. Rev. D* **92** 063015
[22] Zschocke S 2016 *Phys. Rev. D* **93** 103010
[23] Zschocke S 2016 *Phys. Rev. D* **94** 124007
[24] Teyssandier P and Le Poncin-Lafitte C 2008 *Classical and Quantum Gravity* **25** 145020
[25] Le Poncin-Lafitte C and Teyssandier P 2008 *Phys. Rev. D* **77** 044029
[26] Hees A, Bertone S and Le Poncin-Lafitte C 2014 *Phys. Rev. D* **89** 064045
[27] Teyssandier P 2022 arXiv:2212.06671
[28] Linet B and Teyssandier P 2016 *Phys. Rev. D* **93** 044028
[29] Qin C G and Shao C G 2017 *Phys. Rev. D* **96** 024003
[30] Deng X M and Xie Y 2012 *Phys. Rev. D* **86** 044007
[31] Qin C G, Tan Y J, Chen Y F and Shao C G 2019 *Phys. Rev. D* **100** 064063
[32] Hees A, Bertone S and Le Poncin-Lafitte C 2014 *Phys. Rev. D* **90** 084020
[33] Jiang C, Yang B and Lin W 2023 arXiv:2306.10129
[34] Soffel M, Klioner S A, Petit G, *et al.* 2003 *Astronom. J.* **126** 2687
[35] Linet B and Teyssandier P 2002 *Phys. Rev. D* **66** 024045
[36] Müller V 2017 *Hannover: Gottfried Wilhelm Leibniz Universität Hannover*